Anal. Chem. **2004,** *76,* 2798−2806

A Test Field for the Second-Order Advantage in Bilinear Least-Squares and Parallel Factor Analyses: Fluorescence Determination of Ciprofloxacin in Human Urine

Patricia C. Damiani,[†] Alberto J. Nepote,[‡] Mariela Bearzotti,[†] and Alejandro C. Olivieri*,[†]

Cátedra de Química Analítica II, Facultad de Bioquímica y Ciencias Biológicas, Universidad Nacional del Litoral, Paraje El Pozo, Santa Fe (3000), Argentina, and Departamento de Química Analítica, Facultad de Ciencias Bioquímicas y Farmacéuticas, Universidad Nacional de Rosario, Suipacha 531, Rosario (S2002LRK), Argentina

The analytical performances of two algorithms, the recently introduced bilinear least-squares (BLLS) and the popular parallel factor analysis (PARAFAC), are compared as regards second-order fluorescence data recorded for the determination of the fluoroquinolone antibiotic ciprofloxacin in human urine samples. The applied chemometric methodologies employ different strategies for exploiting the so-called second-order advantage, which allows one to obtain individual concentrations of calibrated analytes in the presence of any number of uncalibrated (urine) components. Analysis of a spiked urine test set (in the analyte concentration range 0−200 mg L^{-1}) showed that BLLS provides results of slightly better quality than PARAFAC. Satisfactory results have been obtained on comparing the concentrations predicted for a series of real urine samples with those furnished by liquid chromatography. The limit of detection of the fluorescence-based methods is ∼5 mg L^{-1}.

High-order data are particularly suitable for the quantitative analysis of complex multicomponent samples.[1] In recent years, three-way data following the trilinear model, such as excitation−emission fluorescence matrices (EEM), have been gaining widespread analytical acceptance. Pertinent examples are the determination of therapeutic drugs in biological fluids,[2−5] pesticides,[6] and chlorophylls and pheopigments.[7] The recording of this type of data conveys certain advantages: the measurements are carried out on a single instrument, the signals are selective and sensitive, and the obtained models are trilinear. There are, however, other methods for generating high-order data: UV−visible spectrophotometry coupled to pH or kinetic changes[8,9] and hyphenated techniques such as chromatography coupled to mass spectrometry detection.[10]

In the context of three-way fluorescence analysis, the parallel factor (PARAFAC) model is being increasingly used for data processing,[11,12] because it achieves decomposition of three-dimensional arrays in a unique manner, allowing relative concentrations and spectral profiles of individual sample components to be extracted directly. The term *second-order advantage* has been coined to describe this property, which holds an immense potentiality in the analysis of complex samples.[1] From the analytical point of view, other important characteristics of the PARAFAC methodology are as follows: (1) it avoids the construction of the large training sets needed for the application of first-order multivariate methodologies to complex biological samples (see, for example, the PLS-1 determinations of theophylline,[13] tetracycline,[14] and glucose[15] in human serum) and (2) it handles multiple calibration standards with a pseudounivariate regression plot, in contrast to methods such as generalized rank annihilation (GRAM).[16] It should be noted that the popular multidimensional variant of partial least-squares regression (N-PLS)[17] does not show the second-order advantage, because it is unable to model the occurrence of uncalibrated components in an unknown sample.

Recently, bilinear least squares (BLLS) has been introduced as an appealing second-order chemometric technique, based on a completely different philosophy as compared to PARAFAC and showing the important characteristics of handling multiple standard samples and exploiting the second-order advantage.[18,19] It has been tested using simulated data sets and relatively simple

* To whom correspondence should be addressed. E-mail: aolivier@fbioyf.unr.edu.ar.

[†] Universidad Nacional de Rosario.

[‡] Universidad Nacional del Litoral.

(1) Booksh, K. S.; Kowalski, B. R. *Anal. Chem.* **1994**, *66*, 782A−791A.
(2) Arancibia, J. A.; Escandar, G. M. *Talanta* **2003**, *60*, 1113−1121.
(3) Arancibia, J. A.; Olivieri, A. C.; Escandar, G. M. *Anal. Bioanal. Chem.* **2002**, *374*, 451−459.
(4) Muñoz de la Peña, A.; Espinosa Mansilla, A.; González Gómez, D.; Olivieri, A. C.; Goicoechea, H. C. *Anal. Chem.* **2003**, *75*, 2640−2646.
(5) Trevisan, M. G.; Poppi, R. J. *Anal. Chim. Acta* **2003**, *493*, 69−81.
(6) Rodríguez-Cuesta, M. J.; Boqué, R.; Rius, F. X.; Picón Zamora, D.; Martínez Galera, M.; Garrido Frenich, A. *Anal. Chim. Acta* **2003**, *491*, 47−56.
(7) Moberg, L.; Robertsson, G.; Karlberg B. *Talanta* **2001**, *54*, 161−170.
(8) Espinosa-Mansilla, A.; Muñoz de la Peña, A.; Goicoechea, H. C.; Olivieri, A. C. *Appl. Spectrosc.* **2004**, *58*, 83−90.
(9) Levi, M. A. B.; Scarminio, I. S.; Poppi R. J.; Trevisan M. G. *Talanta* **2004**, *62*, 299−305.
(10) Wilson, I. D.; Brinkman, U. A. Th. *J. Chromatogr., A* **2003**, *1000*, 325−356.
(11) Andersen, C. M.; Bro, R. *J. Chemom*, **2003**, *17*, 200−215.
(12) Bro, R. *Chemom. Intell. Lab. Syst.* **1997**, *38*, 149−171.
(13) Goicoechea, H. C.; Muñoz de la Peña, A.; Olivieri, A. C. *Anal. Chim. Acta* **1999**, *384*, 95−103.
(14) Goicoechea, H. C.; Olivieri, A. C. *Anal. Chem.* **1999**, *71*, 4361−4368.
(15) Zhang, L.; Small, G. W.; Arnold, M. A. *Anal. Chem.* **2002**, *74*, 4097−4108.
(16) Sanchez, E.; Kowalski, B. R. *Anal. Chem.* **1986**, *58*, 496−499.
(17) Bro, R. *J. Chemom*, **1996**, *10*, 47−61.
(18) Linder, M.; Sundberg, R. *Chemom. Intell. Lab. Syst.* **1998**, *42*, 159−178.
(19) Linder, M.; Sundberg, R. *J. Chemom*, **2002**, *16*, 12−27.

10.1021/ac035541w CCC: $27.50
Published on Web 04/14/2004

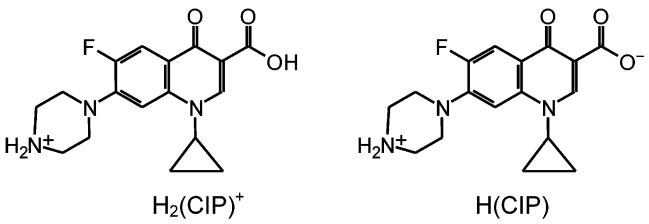

Figure 1. Structures of the two prototropic forms of ciprofloxacin coexisting at pH 6 in aqueous solution.

experimental examples and claimed to give results of at least the same quality as PARAFAC.[19,20] To the best of our knowledge, however, BLLS has not been seriously tested against real samples of high complexity, such as those of biological origin.

In the present report, both BLLS and PARAFAC are employed to predict the concentration of the antibiotic ciprofloxacin in human urine samples from second-order fluorescence data. Ciprofloxacin [1-cyclopropyl-6-fluoro-1,4-dihydro-4-oxo-7-(piperazinyl)quinolone-3-carboxylic acid, Figure 1] is a synthetic fluoroquinolone derivative which has Gram (+) and Gram (−) antibacterial activity[21] and is widely used in the treatment of several bacterial infections in humans and animals.[22,23] Its main excretion pathway is urinary,[24] with usual concentrations in the range 100−200 mg L^{-1}. Following early recommendations,[25] the U.S. Food and Drug Administration (FDA) has approved ciprofloxacin for postexposure inhalational anthrax. High-performance liquid chromatography (HPLC) is regularly employed for routine determination of ciprofloxacin in biological fluids,[26,27] although luminescence techniques coupled to lanthanide sensitization,[28] solid-phase measurements,[29] and multivariate calibration[2] are modern analytical alternatives. Other less employed methods are spectrophotometry,[30] capillary electrophoresis,[31] and conductimetry.[32] Monitoring in body fluids is especially important in children: despite some contraindications, infants and children with multi-drug-resistant infections, cystic fibrosis, or immunological compromise have been successfully treated with ciprofloxacin.[33]

Ciprofloxacin is a weak diprotic acid, which may exist in solution in several prototropic forms.[34] In the present work, fluorescence measurements have been conducted under two different pH conditions: in one case a single acid−base form exists in solution, whereas in the second one an equilibrium occurs between two forms having distinct fluorescent properties. In the former case, the spectral profiles extracted by both of the employed chemometric methods are similar, but in the latter one, there are fundamental differences between PARAFAC and BLLS. This provides an interesting test field where these algorithms can be compared, as regards their model interpretabilities and predictive capabilities toward analytes that are embedded in a complex biological background.

The results are indicative that ciprofloxacin analysis can be conveniently performed in urine samples by second-order fluorescence measurements and that the newly introduced BLLS method is able to yield results that are of a better quality than PARAFAC. In this respect, BLLS deserves a status similar to other well-established second-order calibration methodologies. For comparison, N-PLS results are also included and shown to be unsatisfactory for the presently studied samples.

EXPERIMENTAL SECTION

Equipment. All fluorescence measurements were carried out on an Aminco Bowman Series 2 spectrofluorophotometer, equipped with a 150-W Xe lamp, and connected to a microcomputer running under OS/2 (through a GPIB IEEE-488 interface). Data acquisition was performed by the use of AB2 software. In all cases, 1.00-cm quartz cells were used. EEMs were registered in the ranges λ_{em} = 370−478 nm each 3 nm and λ_{exc} = 250−320 nm each 5 nm, making a total of 37 × 15 = 555 data points per sample matrix. The excitation and emission slit widths were both 4 nm, and the scan rate was 10 nm min^{-1}.

HPLC was performed using a Waters liquid chromatograph equipped with a 515 Waters high-pressure pump, a Rheodyne injector, and an UV−visible detector. Relevant parameters were as follows: column, Zorbax SB C18 4.6 × 150 mm (5-μm particle size); mobile phase, an 87:13 mixture of acetonitrile and H_3PO_4 0.025 M (adjusted to pH 3.0 ± 0.1 with triethanolamine); flow rate, 1 mL min^{-1}; temperature, 25 ± 1 °C; retention time, 10.5 ± 0.1 min. Detection proceeded by absorbance measurements at 280 nm.

Solutions. A stock 53.5 mg L^{-1} solution of analytical grade ciprofloxacin (Sigma) was prepared by dissolving the compound in a 50:50 mixture of ethanol and doubly distilled water, sonicating for at least 30 min. and storing in the dark at 4 °C. Working solutions were prepared by dilution of the stock solution with either a sodium acetate buffer (pH 4.0) or with doubly distilled water (pH ∼6). The degree of dilution was such that the maximum proportion of ethanol in the final solutions was less than 0.2%.

Calibration Samples. The linear fluorescence−concentration range for ciprofloxacin was previously checked to have an upper limit of 260 μg L^{-1}. Calibration was thus performed with five aqueous solutions of ciprofloxacin, having equally spaced concentrations in the range 0−200 μg L^{-1}. They were prepared by appropriate dilution of the analyte stock solution. Two different calibration sets were prepared, one kept at pH 4.0 by means of

(20) Linder, M. Bilinear Regression and Second-Order Calibration. Doctoral Thesis, Stockholm University, Sweden, 1998.
(21) Jackson, L. C.; Machado, L. A.; Hamilton, M. L. *Acta Med.* **1998**, *8*, 58−61.
(22) Ihrke, P. J.; Papich, M. G.; Demanuelle, T. C. *Vet. Dermatol.* **1999**, *10*, 193−204.
(23) Chen, D. K.; McGeer, A.; de Azavedo, J. C.; Low, D. E. *N. Engl. J. Med.* **1999**, *341*, 233−239.
(24) Suthakaran, C.; Adithan, C.; Rajaram, S.; Shashindran, C. H.; Tripathi K. D.; Gandhi, I. S. *Indian J. Pharmacol.* **1992**, *24*, 25−28.
(25) Inglesby, T. V.; Henderson, D. A.; Bartlett, J. G.; Ascher, M. S.; Eitzen, E.; Friedlander, A. M.; Hauer, J.; McDade, J.; Osterholm, M. T.; O'Toole, T.; Parker, G.; Perl, T. M.; Russell, P. K.; Tonat, K. *J. Am. Med. Assoc.* **1999**, *281*, 1735−1745.
(26) Ballesteros, O.; Toro, I.; Sanz-Nebot, V.; Navalón, A.; Vílchez J. L.; Barbosa J. *J. Chromatogr.* **2003**, *798*, 137−144.
(27) Krol, G. J.; Beck G. W.; Benham T. *J. Pharm. Biomed. Anal.* **1995**, *14*, 181−190.
(28) Rodríguez-Díaz, R. C.; Aguilar-Caballos M. P.; Gómez-Hens A. *Anal. Chim. Acta* **2003**, *494*, 55−62.
(29) Navalón, A.; Ballesteros, O.; Blanc, R.; Vílchez, J. L. *Talanta* **2000**, *52*, 845−852.
(30) Mostafa, S.; El Sadek, M.; Alla, E. A. *J. Pharm. Biomed. Anal.* **2002**, *27*, 133−142.
(31) Barron, D.; Jimenez Lozano, E.; Cano, J.; Barbosa, J. *J. Chromatogr., B Biomed. Appl.* **2001**, *759*, 73−79.
(32) Issa, Y. M.; El-Hawary, W. F.; Ahmed, A. F. *Mikrochim. Acta* **2000**, *134*, 9−14.
(33) Echols, R. M. *Pediatr. Infect. Dis. J.* **1997**, *16*, 89−90.
(34) Drakopoulos, A. I.; Ioannou, P. C. *Anal. Chim. Acta* **1997**, *354*, 197−204.

Table 1. N-PLS, PARAFAC, and BLLS Prediction Results on the Spiked Urine Test Set[a]

		PARAFAC		BLLS		N-PLS[b]	
sample	nominal	pH 4.0	pH 6[c]	pH 4.0	pH 6	pH 4.0	pH 6
T1	190	203	173	194	214	203	208
T2	87	96	80	94	86	100	107
T3	23	33	26	32	29	43	46
T4	13	14	6	15	14	27	28
T5	38	34	19	36	28	48	50
T6	150	153	142	154	145	165	160
T7	26	32	33	34	16	48	47
T8	58	63	67	65	60	77	80
T9	125	131	146	132	126	143	146
T10	65	62	63	64	67	77	75
T11	90	85	89	87	92	101	120
T12	160	158	158	158	172	173	174
T13	48	48	41	47	52	58	61
T14	75	79	64	76	68	88	92
T15	0	−1	10	−1	11	13	26
T16	0	−1	5	−1	8	16	21
T17	0	2	3	0	7	15	30
T18	0	−4	11	−3	7	14	27

[a] All results are expressed in μg L^{-1}, corresponding to values 1000 times larger in the original urines. [b] The N-PLS model was built with a single factor at both pH values, as obtained from leave-one-out cross-validation. [c] Values were computed using data for the most sensitive prototropic $H_2(CIP)^+$ form.

an acetate buffer and a second one at pH 6 (provided by a significant dilution with doubly distilled water). The range of calibration concentrations corresponds to values between 0 and 200 mg L^{-1} when converted to undiluted urine samples (see below). EEM recording was performed in random order with respect to the sample number.

Spiked Test Samples. Four different urine samples, taken from healthy individuals, were used to generate 14 spiked test samples. Each urine sample was added to the analyte in order to obtain a final concentration of ciprofloxacin, which was selected at random from the corresponding calibration range. Addition of the four urine blanks to this set led to an 18-test sample set for analyzing the method's performance (see concentrations in Table 1). Ciprofloxacin was added to the urines from the working solution (as required) and diluted (1:1000). In one set, the pH was maintained at 4.0 (dilution was made with an acetate buffer), and in a separate set, the pH was ~6 (dilution was made with doubly distilled water). EEM recording was performed in random order with respect to sample number and on different days (i.e., samples were divided into three subsets, and EEM for samples in each subset were run in three consecutive days).

Urine Samples. Real urine samples were taken from patients administered with ciprofloxacin and obtained at a regional hospital. They were diluted (1:1000) with the acetate buffer of pH 4.0 or with water, to bring the concentration of the analyte into the calibration range, and the EEMs were read. The multivariate strategies PARAFAC and BLLS were applied at both pH values. Samples were also studied using the HPLC technique for comparison with the fluorescent methodologies.

Chromatographic Procedure. It is based on the method described in the *United States Pharmacopeia*.[35] A standard solution of ciprofloxacin (180 mg L^{-1}) was prepared by dissolving the compound in the mobile phase (see above). Real urine samples were diluted (1:2) with mobile phase in order to obtain concentrations in the range 80−120 mg L^{-1}. In all cases, triplicate analysis was performed.

THEORY

PARAFAC. Second-order data are obtained when a given sample produces a $J \times K$ data matrix or second-order array, where J and K denote the number of data points in the first and second dimensions, respectively (in EEM fluorescence measurements, J is the number of digitized emission wavelengths and K is the number of excitation wavelengths). If the I training matrices and the unknown sample matrix are stacked, a three-way data array $\boldsymbol{X}$ is obtained, whose dimensions are $[(I + 1) \times J \times K]$. Provided $\boldsymbol{X}$ follows the trilinear PARAFAC model, it can be written as a sum of Kronecker products of three vectors for each responsive component: $\mathbf{a}_n$, $\mathbf{b}_n$, and $\mathbf{c}_n$, which collect the relative concentrations or scores $[(I + 1) \times 1]$, the emission profiles $(J \times 1)$, and the excitation profiles $(K \times 1)$ for component n, respectively. The specific expression is thus[36]

$$\mathbf{X} = \sum_{n=1}^{N} \mathbf{a}_n \otimes \mathbf{b}_n \otimes \mathbf{c}_n + \mathbf{E} \qquad (1)$$

where ⊗ indicates the well-known Kronecker product, N is the total number of responsive components, and $\boldsymbol{E}$ is a residual error term of the same dimensions as $\boldsymbol{X}$. The column vectors $\mathbf{a}_n$, $\mathbf{b}_n$, and $\mathbf{c}_n$ are usually collected into the loading matrices **A**, **B**, and **C**, respectively.

The model described by eq 1 defines a decomposition of $\boldsymbol{X}$, which provides access to spectral profiles (**B** and **C**) and relative concentrations (**A**) of individual components in the $(I + 1)$ mixtures, whether they are chemically known or not, constituting the basis of the second-order advantage. The decomposition is accomplished by PARAFAC through an alternating least-squares minimization.[12,37]

Issues relevant to the application of the PARAFAC model to three-way fluorescent data are as follows: (1) initializing and/or constraining the algorithm, (2) establishing the number of fluorophores and the reliability of the model, (3) identifying specific fluorescent components from the information provided by the model, and (4) calibrating the model in order to obtain absolute concentrations for a particular component in an unknown sample.

Initialization of the least-squares fit can be carried out with profiles obtained by several procedures. The most usual one is direct trilinear decomposition,[38] but in certain instances, special procedures are required.[39] Furthermore, depending on the characteristics of the studied system, constraints should be applied to the PARAFAC loadings in order to obtain physically meaningful information.

The number of responsive components (N) can be estimated by several methods. A useful technique is the consideration of the PARAFAC internal parameter known as core consistency: typically, the latter one is computed for a number of trial

(35) *United States Pharmacopeia XXIV*, United States Pharmacopeial Convention: Rockville, MD, 2000; pp 417−420.

(36) Leurgans, S.; Ross, R. T. *Stat. Sci.* **1992**, *7*, 289−319.
(37) Paatero, P. *Chemom. Intell. Lab. Syst.* **1997**, *38*, 223−242.
(38) Sánchez, E.; Kowalski, B. R. *J. Chemom.* **1990**, *4*, 29−45.
(39) Bro, R. Multi-way analysis in the food industry. Doctoral Thesis, University of Amsterdam, The Netherlands, 1998.

components, and N is set as one less the number for which the core consistency drops from ~100 to less than 50.[39] An intuitive alternative method is based on the pseudounivariate calibration line, which is obtained by regressing the PARAFAC relative concentration values for the training samples against their standard concentrations.[4] The correct value of N is easily located when the linear fit regression error stabilizes as a function of a number of trial components: when the correct number of constituents is reached, the PARAFAC relative concentrations for a given component are linearly related to its nominal concentrations. Introducing more components should lead to a similar (or possibly worse) fit. A PARAFAC model constructed with the correct number of components is deemed to be correct if a reasonably low number of least-squares errors, i.e., elements of **E** in eq 1, are obtained in comparison with the instrumental noise level.

Identification of the chemical constituent under investigation is done with the aid of the spectral profiles **B** and **C**, as extracted by PARAFAC, and comparing them with those for a standard solution of the analyte of interest. This is required since the components obtained by decomposition of $\boldsymbol{X}$ are sorted according to their contribution to the overall spectral variance, and this order is not necessarily maintained when the unknown sample is changed.

Absolute analyte concentrations are obtained after proper calibration, since only relative values (**A**) are provided by decomposing the three-way data array. Experimentally, this is done by preparing a set of standards of known composition and regressing the first I elements of column $\mathbf{a}_n$ against known standard concentrations **y** of analyte n:

$$k = \mathbf{y}^{+} \times [a_{1n} \mid \ldots \mid a_{In}] \tag{2}$$

where "+" implies taking the pseudoinverse.

Finally, conversion of relative to absolute concentration of n in the unknown is achieved from the last element of column $\mathbf{a}_n$ $[a_{(I+1)n}]$ and the slope of the calibration graph k:

$$y_u = a_{(I+1)n}/k \tag{3}$$

In sum, the most salient point of the PARAFAC philosophy is the construction of a joint model that includes the data matrices for the I calibration samples together with that for the unknown sample, before concentration information is introduced in a separate pseudounivariate regression step.

BLLS. The original BLLS formulation is discussed in detail in the relevant references.[18,19] A brief description is presented here, illustrating a general scheme (appropriate for several calibrated analytes) in order to compare with literature information, with the corresponding changes for a single calibrated analyte introduced as required.

In contrast to PARAFAC, concentration information is introduced into the BLLS calibration step (without including data for the unknown sample), to obtain approximations to pure analyte matrices at unit concentration. For this purpose, the concentration product matrix **D** and N_{cal} concentration-weighted $\mathbf{T}_n$ matrices are first obtained (N_{cal} is the number of calibrated analytes), employing data from the I training matrices $\mathbf{X}_{i,cal}$ and the calibrated analyte concentrations contained in the $I \times N_{cal}$ matrix **Y**:

$$\mathbf{T}_n = \sum_{i=1}^{I} Y_{in}\mathbf{X}_{i,cal} \tag{4}$$

$$\mathbf{D} = \mathbf{Y}^{T}\,\mathbf{Y} \tag{5}$$

The required $\mathbf{S}_n$ matrices for analyte n at unit concentration are then obtained as

$$\mathbf{S}_n = \sum_{n'=1}^{N} (D^{-1})_{nn'}\mathbf{T}_{n'} \tag{6}$$

Notice that in the presently studied analytical problem, a single calibrated analyte occurs. Hence, $N_{cal} = 1$, $n = 1$, and $\mathbf{T}_n$ should be replaced by $\mathbf{T}_1$, **Y** by the vector **y** of known standard concentrations, as used above for PARAFAC, **D** by the scalar quantity D, and $\mathbf{S}_n$ by $\mathbf{S}_1$:

$$\mathbf{T}_1 = \sum_{i=1}^{I} y_i\mathbf{X}_{i,cal} \tag{7}$$

$$D = \mathbf{y}^{T}\,\mathbf{y} \tag{8}$$

$$\mathbf{S}_1 = \sum_{n'=1}^{N} D^{-1}\mathbf{T}_1 \tag{9}$$

The $J \times K$ matrices $\mathbf{S}_n$ ($\mathbf{S}_1$ in our case) allow one to estimate the calibrated analyte spectral profiles. Two procedures have been discussed for this purpose: the BLLS profile estimator and the singular value decomposition (SVD) profile estimator; the most reliable and simple seems to be the single-component SVD of each of the $\mathbf{S}_n$ (SVD_1):[18,19]

$$\mathbf{b}_n g_n \mathbf{c}_n^{T} = \mathrm{SVD}_1(\mathbf{S}_n) \tag{10}$$

where $\mathbf{b}_n$ and $\mathbf{c}_n$ are the emission ($J \times 1$) and excitation ($K \times 1$) profiles. In the present case eq 10 reduces to

$$\mathbf{b}_1 g_1 \mathbf{c}_1^{T} = \mathrm{SVD}_1(\mathbf{S}_1) \tag{11}$$

In general, where more than one analyte is calibrated, the profiles provided by eq 10 are joined into the calibration $\mathbf{B}_{cal}$ and $\mathbf{C}_{cal}$ loading matrices, similar to those described above for PARAFAC, except that they do not include possible unexpected components that may appear in the unknown sample. In our case, however, $\mathbf{B}_{cal} = \mathbf{b}_1$ and $\mathbf{C}_{cal} = \mathbf{c}_1$. It should be noted that the identification of calibrated components is not required in BLLS, since this is automatically performed by the algorithm.

If the calibration model is exact, $\mathbf{B}_{cal}$ and $\mathbf{C}_{cal}$ can be employed to estimate the analyte concentrations in the unknown. As previously discussed,[18,19] there are two procedures for this prupose, a so-called naive predictor and a least-squares predictor. The latter one has been shown to be more reliable and leads to the following prediction equation:[18,19]

$$\mathbf{y}_u = [(\mathbf{B}_{cal}^{T}\mathbf{B}_{cal}) * (\mathbf{C}_{cal}^{T}\mathbf{C}_{cal})]^{-1}\,\mathrm{Diag}(\mathbf{B}_{cal}^{T}\mathbf{X}_u\mathbf{C}_{cal}) \tag{12}$$

where $\mathbf{y}_u$ is an $N_{cal} \times 1$ vector containing the predicted concentrations of the calibrated N_{cal} analytes, * indicates the elementwise product operation, $\mathbf{X}_u$ is the unknown data matrix, and Diag converts the main diagonal of the $N_{cal} \times N_{cal}$ matrix ($\mathbf{B}_{cal}{}^T\mathbf{X}_u\mathbf{C}_{cal}$) into an $N_{cal} \times 1$ vector. Applied to the presently studied problem, eq 12 thus provides the single analyte concentration y_u in the unknown:

$$y_u = [(\mathbf{b}_1{}^T\mathbf{b}_1) * (\mathbf{c}_1{}^T\mathbf{c}_1)]^{-1}\,\mathrm{Diag}(\mathbf{b}_1{}^T\mathbf{X}_u\mathbf{c}_1) \qquad (13)$$

The occurrence of unmodeled compounds in an unknown sample is investigated by comparing the residuals of the prediction least-squares fit with the instrumental noise level (the latter is easily assessed by blank replication measurements). If unexpected components indeed occur, the situation is handled by a separate iterative procedure called residual bilinearization (RBL),[18,19] which in a general case would be carried out according to the following steps:

(1) Set $N_{int} = 1$ as a trial number of interfering components contained in the unknown sample.

(2) Calculate $\mathbf{y}_u$ with eq 14 and the matrix $\mathbf{E}_u$ of positive residuals for the prediction step with eq 15 (the first time this RBL procedure is used, set $\mathbf{B} = \mathbf{B}_{cal}$ and $\mathbf{C} = \mathbf{C}_{cal}$):

$$\mathbf{y}_u = [(\mathbf{B}^T\mathbf{B})^{-1} * (\mathbf{C}^T\mathbf{C})^{-1}]\,\mathrm{Diag}(\mathbf{B}^T\mathbf{X}_u\mathbf{C}) \qquad (14)$$

$$\mathbf{E}_u = |\,\mathbf{X}_u - \mathbf{B}\mathbf{Y}_u\mathbf{C}^T\,| \qquad (15)$$

where $\mathbf{Y}_u$ is a diagonal matrix whose diagonal elements are those of $\mathbf{y}_u$ and the remaining ones are zeros.

(3) Perform SVD with N_{int} components on the matrix $\mathbf{E}_u$ and obtain the profiles for the interference(s):

$$\mathbf{B}_{int}\mathbf{G}_{int}\mathbf{C}_{int}{}^T = \mathrm{SVD}_{Nint}(\mathbf{E}_u) \qquad (16)$$

(4) Expand the profiles to include $\mathbf{B}_{int}$ and $\mathbf{C}_{int}$:

$$\mathbf{B} = [\mathbf{B}_{cal} \mid \mathbf{B}_{int}] \qquad (17)$$

$$\mathbf{C} = [\mathbf{C}_{cal} \mid \mathbf{C}_{int}] \qquad (18)$$

(5) Return to step 2 and continue until convergence.

(6) If the residuals are still significantly larger than the noise level, return to step 1 and increase the number of interferences by one. Notice that the final value of N in BLLS is given by $N_{cal} + N_{int}$.

The above procedure, as adapted to the present problem with a single calibrated analyte, requires the replacement of $\mathbf{B}_{cal}$ by $\mathbf{b}_1$, $\mathbf{C}_{cal}$ by $\mathbf{c}_1$, and both $\mathbf{y}_u$ and $\mathbf{Y}_u$ by y_u.

The prevailing idea within BLLS is a two-step calibration-prediction mode, where concentration prediction is guided by a least-squares minimization. The second-order advantage is left for a subsequent stage, in which the matrix residuals are bilinearized in order to estimate the interference profiles. The latter serve to expand the loadings and to correctly estimate the analyte concentrations, even in the presence of unexpected constituents. Notice that no initialization or constraining procedures are required.

Figures of Merit. Figures of merit are regularly employed for method comparison. They are best understood by resorting to the useful concept of net analyte signal (NAS), first developed by Lorber.[40] In multivariate calibration, the NAS usually takes the following form:

$$\mathbf{x}_n{}^* = \mathbf{P}_{NAS}\,\mathrm{vec}(\mathbf{X}_u) \qquad (19)$$

where $\mathbf{x}_n{}^*$ is the NAS vector, $\mathbf{P}_{NAS}$ is a $JK \times JK$ projection matrix, and vec is an operator that unfolds the matrix $\mathbf{X}_u$ columnwise into a vector. There appears to be conflicting reports as how the NAS projection should be computed for higher order methodologies.[41−44] An equation that seems to be appropriate for cases where the second-order advantage operates is[43]

$$\mathbf{P}_{NAS} = [\mathbf{I} - \mathbf{B}_{-n}(\mathbf{B}_{-n})^+] \otimes [\mathbf{I} - \mathbf{C}_{-n}(\mathbf{C}_{-n})^+] \qquad (20)$$

where $\mathbf{I}$ is an appropriately dimensioned unit matrix and $\mathbf{B}_{-n}$ and $\mathbf{C}_{-n}$ are the $\mathbf{B}$ and $\mathbf{C}$ matrices from which the columns corresponding to analyte n have been removed. The sensitivity can then be defined as the scalar NAS at unit concentration:[43]

$$\mathrm{SEN} = [\mathrm{Tr}(\mathbf{x}_n{}^{*T}\mathbf{x}_n{}^*)]^{1/2}/y_u \qquad (21)$$

where y_u is the predicted concentration for a given analyte in the sample and Tr indicates taking the trace of a matrix. Equation 21 is equivalent to[45]

$$\mathrm{SEN} = k\,\{[(\mathbf{B}^T\mathbf{B})^{-1}]_{nn}\,[(\mathbf{C}^T\mathbf{C})^{-1}]_{nn}\}^{1/2} \qquad (22)$$

where k is an appropriate scaling factor. In PARAFAC, k is the parameter converting scores to concentrations (eq 2), while in BLLS it can be obtained by regressing the g_1 values (eq 11) against $\mathbf{y}$.

The selectivity (SEL), in turn, is the ratio between the sensitivity and the total signal, and can be estimated as[45]

$$\mathrm{SEL} = \{[(\mathbf{B}^T\mathbf{B})^{-1}]_{nn}\,[(\mathbf{C}^T\mathbf{C})^{-1}]_{nn}\}^{1/2} \qquad (23)$$

Note that when the second-order advantage is employed, eqs 22 and 23 imply that SEN and SEL are sample-specific and cannot be defined for the multivariate method as a whole. In such cases, average values for a set of samples can be estimated and reported.

A further figure of merit is the standard error in the predicted concentrations, an area of active research in the second-order

(40) Lorber, A. *Anal. Chem.* **1986**, *58*, 1167−1172.
(41) Messick, N. J.; Kalivas J. H.; Lang, P. M. *Anal. Chem.* **1996**, *68*, 1572−1579.
(42) Wang, Y.; Borgen, O. S.; Kowalski, B. R.; Gu M.; Turecek, F. *J. Chemom.* **1993**, *7*, 117−130.
(43) Faber, K.; Lorber, A.; Kowalski B. R. *J. Chemom.* **1997**, *11*, 419−461.
(44) Ho, C.-N.; Christian G. D.; Davidson, E. R. *Anal. Chem.* **1980**, *52*, 1071−1079.
(45) Faber, N. M. *J. Chemom.* **2001**, *15*, 743−748.

calibration scenario. Mathematical expressions for sample-specific prediction uncertainties take proper account of the propagation of different error sources. They are available for PARAFAC[46] and BLLS,[19] although for cases not exploiting the second-order advantage, and hence, they are not applicable to the present example. A useful alternative is to resort to mean prediction errors for a set of test samples, to obtain an average concentration error, useful for method comparison (see below). Further insight into the accuracy and precision of the method is gained by linearly regressing predicted versus nominal concentration values in the test sample set and finding the so-called elliptical joint region (EJCR) for the regression slope and intercept.[47] If the theoretical point (i.e., slope 1, intercept 0) is included into the EJCR, the method is considered to be accurate, while the size of the ellipse gives an idea of the precision.[47]

Finally, the limit of detection (LOD) should be considered. This figure of merit has been recently discussed for several first- and second-order multivariate techniques, using a rigorous approach that takes into account false positive and false negative errors.[48,49] In the case of PARAFAC, a recent work has discussed the estimation of the LOD, but only in situations where the second-order advantage is not operating, i.e., when all components present in unknown samples have been calibrated.[46] Thus, the latter approach is not strictly applicable to the present problem. An approximation to the LOD can still be gathered from the expression[46]

$$\mathrm{LOD} = 3\, s_r / \mathrm{SEN} \qquad (24)$$

where s_r is the instrumental noise level. Equation 24 stems from the consideration of a signal-to-noise ratio equal to 3 but does not account for calibration uncertainties, and thus, it generally provides overoptimistic values. Inasmuch as SEN is given as an average value over a test sample set, LOD is also reported as an average figure.

Software. All calculations were done using MATLAB 6.0.[50] Appropriate routines for applying PARAFAC and N-PLS, developed by Bro, are available on the Internet,[51] although a useful MATLAB graphical interface was developed in our laboratory for its implementation, of the type already described for first-order multivariate calibration.[52] It also implements the BLLS method, in this case following the algorithm described in refs 18 and 19. The interface provides a simple means of loading the data matrices into the MATLAB working space, selecting appropriate working spectral regions, and plotting spectral profiles and pseudounivariate calibration graphs. The analytically relevant results are conveniently shown in terms of predicted concentration and figures of merit. This MATLAB interface code is available from the authors on request.

(46) Olivieri, A. C.; Faber, N. M. *Chemom. Intell. Lab. Syst.* **2004**, *70*, 75−82.
(47) González, A. G.; Herrador, M. A.; Asuero, A. G. *Talanta* **1999**, *48*, 729−736.
(48) Boqué, R.; Larrechi, M. S.; Rius, F. X. *Chemom. Intell. Lab. Syst.* **1999**, *45*, 397−408.
(49) Boqué, R.; Ferré, J.; Faber, N. M.; Rius, F. X. *Anal. Chim. Acta* **2002**, *451*, 313−321.
(50) MATLAB 6.0, The MathWorks Inc., Natick, MA, 2000.
(51) http://www.models.kvl.dk/source/
(52) Goicoechea, H. C.; Iñon, F. A.; Olivieri, A. C. *Chemom. Intell. Lab. Syst.* In press.

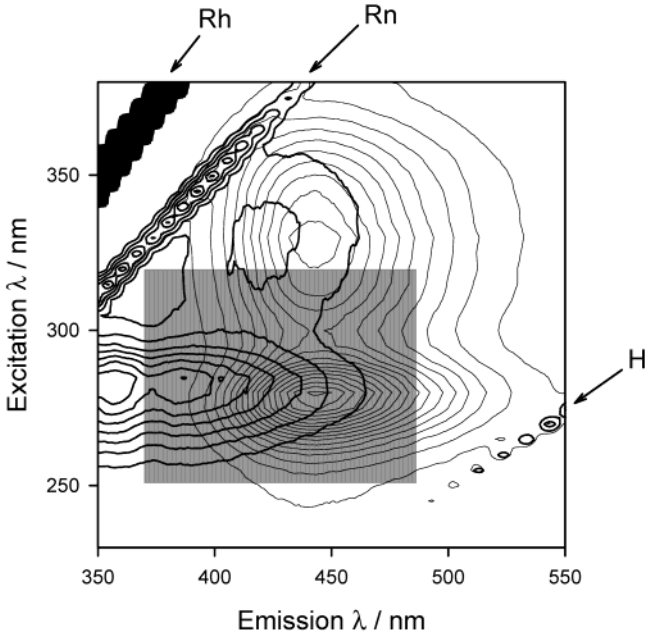

Figure 2. Contour plot of the EEM for an aqueous solution of ciprofloxacin 100.0 μg L^{-1} (narrow lines) and a typical human urine sample diluted 1:1000 (thick lines), showing the presence of a diffraction grating harmonics (H) and Rayleigh (Rh) and Raman (Rn) scatterings, as indicated. The gray rectangle illustrates the spectral excitation and emission ranges selected for calibration with PARAFAC and BLLS.

RESULTS AND DISCUSSION

Excitation−Emission Fluorescence Matrices. As explained above, to test the performances of PARAFAC and BLLS under different conditions, measurements have been made at pH 4.0, where the analyte is mainly present in the protonated form $H_2(CIP)^+$, and also at pH 6, where an acid−base equilibrium occurs between $H_2(CIP)^+$ and the neutral form H(CIP) (most probably a zwitterion), because the relevant ionization pK_a is 5.90 (see Figure 1).[34] Both $H_2(CIP)^+$ and H(CIP) are fluorescent but display different excitation and emission profiles. It should be noted that ciprofloxacin is also able to exist in a further protonated form $H_3(CIP)^{2+}$ in a strongly acid medium, and in the fully deprotonated form (CIP)- in strongly alkaline media.[34] These latter species, however, display low fluorescence intensities and therefore they are not suitable for the analyte determination.

Figure 2 shows the superimposed contour plots corresponding to the EEM for one of the training samples (containing ciprofloxacin 100 μg L^{-1}) and for a typical human urine, both recorded in wide spectral excitation and emission ranges: 230−380 and 350−550 nm, respectively. The presence of both Rayleigh and Raman scatterings is observed, as well as a second harmonic from the diffraction grating, which should be avoided because they are uncorrelated with the target concentrations of the studied analyte. Therefore, for calibration and prediction purposes, the EEMs were subsequently recorded in the sensibly restricted excitation and emission ranges shown as a gray rectangle in Figure 2, which includes the analyte fluorescence peak of highest intensity. This range corresponds to emission from 370 to 478 nm at 3-nm intervals ($J = 37$ data points) and excitation from 250 to 320 nm at 5-nm intervals ($K = 15$ data points), making a total of 555 spectral points per sample matrix. Figure 2 also highlights the

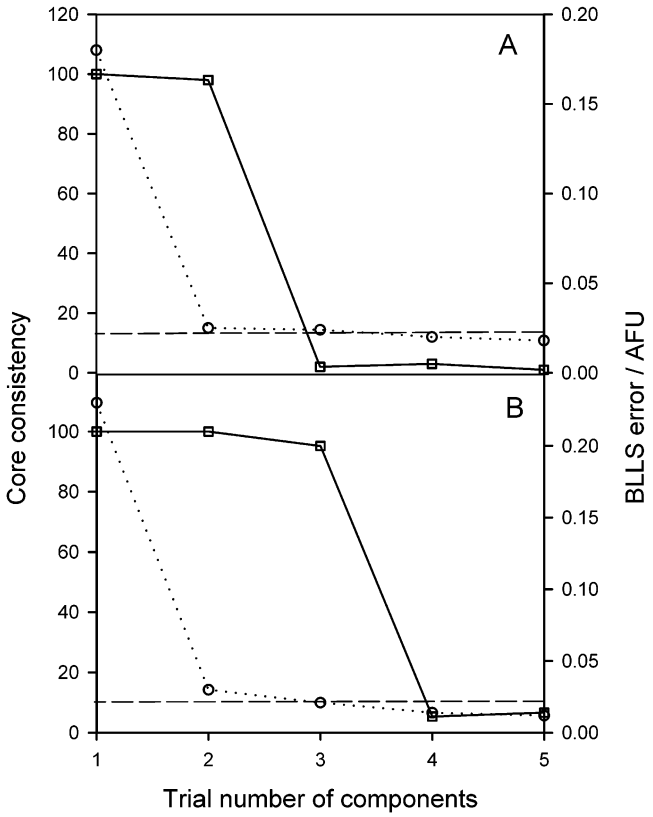

Figure 3. (A) PARAFAC core consistency values (squares) and BLLS least-squares error (circles) as a function of the trial number of components for the analysis of the spiked test sample T1 at pH 4.0. The solid and dotted lines connecting the points (PARAFAC and BLLS, respectively) are for the eye guide. (B) As in plot A for the same test sample studied at pH 6. The horizontal dashed line indicates the average instrumental noise level. AFU, arbitrary fluorescence units.

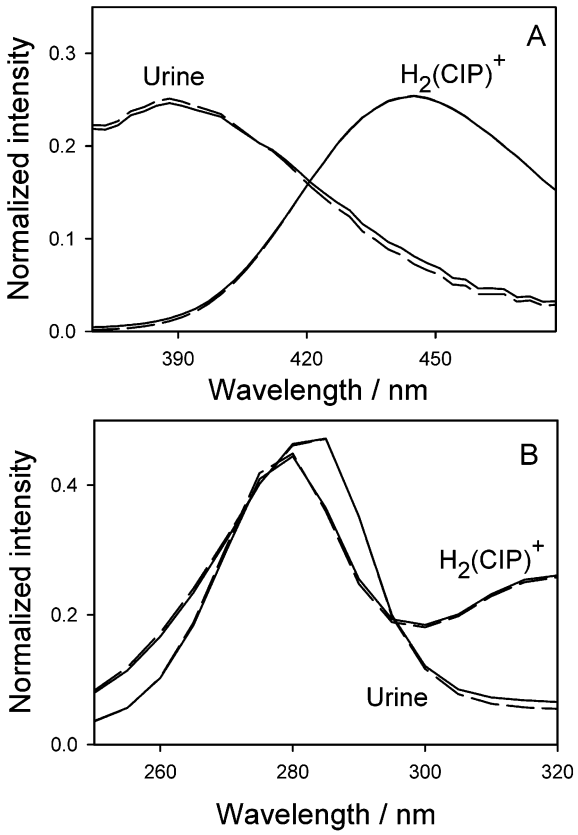

Figure 4. (A) Emission profiles, normalized to unit length, as found by PARAFAC (—) and by BLLS (– –), after processing one the spiked urine test sample T1 at pH 4.0. (B) Excitation profiles. Both in (A) and in (B), the profiles for $H_2(CIP)^+$ were identified by comparison with a standard, with the remaining ones corresponding to the urine background (as indicated).

fact that a significant overlapping occurs between the analyte and the urine background of this particular sample across the examined spectral ranges. It should be noticed that the intensity and spectral shapes of urine vary among different individuals, making if difficult to employ first-order multivariate techniques for ciprofloxacin monitoring, because they are sensitive to unmodeled components. The overlapping situation at pH 6 (not shown) is similar to that described above.

Test Samples. Profile Estimation. The set of 18 test urine samples (14 were spiked with random concentrations of ciprofloxacin and 4 were left as blanks) was investigated with the aid of PARAFAC at pH 4.0. Initialization was performed by direct trilinear decomposition of the three-way array composed by the five training samples and each of the unknown ones, and unconstrained least-squares fit was then carried out. In all cases, core consistency analysis allowed to establish that the appropriate number of fluorophores was two (see Figure 3 for sample T1): one corresponding to ciprofloxacin and the remaining one to the urine background. The use of the pseudounivariate regression criterion led to similar results concerning the number of fluorophores. The fact the urine is modeled with a single component by the algorithm may imply that a major, highly fluorescent component dominates the urine background. Increasing the number of fluorophores does not improve the model fit and leads to poorly defined spectral profiles for the extra components.

The obtained emission and excitation profiles of the two-component model (see Figure 4) nicely match those expected for a pure analyte standard at the working pH value.[34] In all cases, residual least-squares errors were comparable to the instrumental noise, indicating a good fit to the proposed PARAFAC model. BLLS was then applied to the same set. In all samples, the study of the prediction residuals led to the conclusion that further components (in addition to ciprofloxacin) were required to improve the fit. Thus, to apply the RBL procedure, replication of blank samples was performed to obtain an average instrumental noise level of ~0.02 (arbitrary fluorescence units). Figure 3 shows that the BLLS fit error in the case of sample T1 stabilizes at two constituents, in agreement with the PARAFAC results. Furthermore, the spectral profiles provided by RBL for the analyte and for the urine background (Figure 4) are also similar to those furnished by PARAFAC. This result allows one to conclude that BLLS is successful in obtaining profiles for exploiting the second-order advantage.

In going to pH 6, an entirely different situation arises as regards profile estimation. Analysis of the spiked urine set using PARAFAC leads to the conclusion that three responsive components occur at this pH, based on core consistency values (results for sample T1 are provided in Figure 3). According to the obtained profiles, two of them were correctly assigned to $H_2(CIP)^+$ and H(CIP) forms of ciprofloxacin, leaving the remaining one to the urine background (Figure 5). The profiles for the protonated $H_2(CIP)^+$

Table 2. Figures of Merit for PARAFAC and BLLS at Both Studied pH Values[a]

	PARAFAC		BLLS	
parameter	pH 4.0	pH 6	pH 4.0	pH 6
no. of training samples	5			
calibration concn range	0−200 μg L^{-1} (five equally spaced values)			
no. of test samples	18			
test concn range	0−190 μg L^{-1} (random design)			
data structure	one 37 × 15 × 6 three-way array for each unknown		five training 37 × 15 matrices and one matrix for the unknown	
RMSEP[b]/μg L^{-1}	6	10	5	9
sensitivity[b,c]/AFU L μg^{-1}	0.04	0.012	0.04	0.05
selectivity[b]	0.25	0.11	0.26	0.46
LOD[b,c]/μg L^{-1}	2	5	2	1

[a] RMSEP, root-mean-square error of prediction; AFU, arbitrary fluorescence units. The relative prediction error is numerically identical to the RMSEP, since the mean calibration concentration is 100 μg L^{-1}. [b] In the case of PARAFAC at pH 6, the quoted values were computed using data for the most sensitive prototropic $H_2(CIP)^+$ form. [c] Average values over the 18-sample test set, assuming $s_r = 0.02$ AFU.

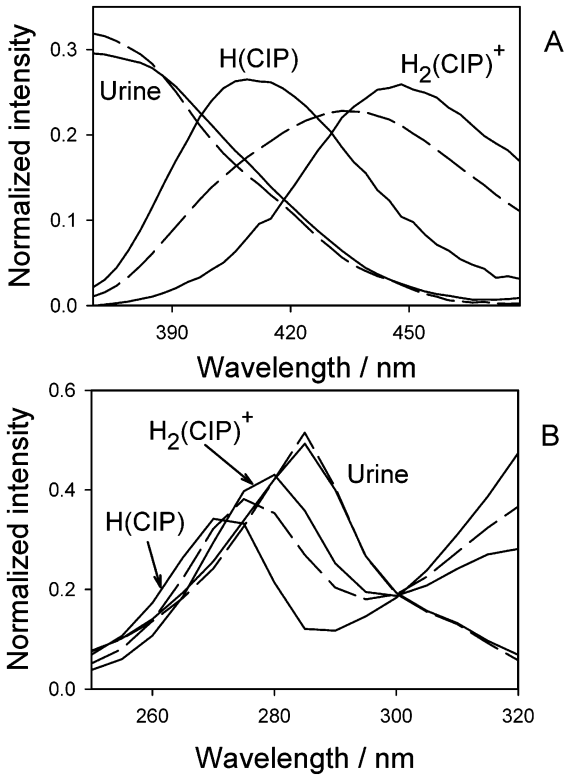

Figure 5. (A) Emission profiles, normalized to unit length, as found by PARAFAC (—) and by BLLS (– –), after processing sample T1 at pH 6. (B) Excitation profiles. Both in (A) and in (B), the PARAFAC profiles for $H_2(CIP)^+$ and H(CIP) were identified by comparison with a standard, the BLLS ones correspond to population averages of those for $H_2(CIP)^+$ and H(CIP), and the remaining one is ascribed to the urine background (as indicated).

form are coincident with those found at pH 4.0 (see Figure 4). It should be noted that at pH 6 the PARAFAC scores for $H_2(CIP)^+$ and H(CIP) components (i.e., the corresponding columns of the **A** matrix) are linearly related. Therefore, the least-squares procedure had to be carried out including a nonnegativity constrain on the three PARAFAC modes, to obtain physically meaningful spectral profiles.[39]

In the case of the application of BLLS, this algorithm yields excitation and emission profiles for the only calibrated component, regardless of its acid−base equilibrium forms, and requiring no particular constrains. The obtained spectral profiles for sample T1 are compared with those rendered by PARAFAC in Figure 5 and are seen to be population averages of those corresponding to $H_2(CIP)^+$ and H(CIP) forms. This is understandable on the basis of the details of the BLLS calibration discussed above: the pure analyte matrix is in this case a compromise between those for the equilibrating species at pH 6. On the other hand, error analysis during the prediction step (Figure 3) indicated the need of an extra component, the urine background. The latter one was found by applying RBL, leading to the profile shown in Figure 5, in pleasing agreement with that found by PARAFAC.

Test Samples. Figures of Merit. Prediction results for the spiked test set are presented in Table 1. In the case of PARAFAC at pH 6, the calibration scheme leads to two separate pseudounivariate regression plots, based on each of the equilibrating prototropic forms of the analyte. The analyte concentration was predicted using data for the most sensitive form $H_2(CIP)^+$. On the other hand, prediction with BLLS is possible using population-averaged profiles in eq 13. All predictions are seen to be reasonable for samples of the complexity of human urine. As regards N-PLS, poor recoveries have been obtained, due to the nonavailability of the second-order advantage for the latter technique: all predicted values are in excess over the nominal ones, by an average of 15 and 19 μg L^{-1} at pH 4.0 and 6, respectively. This is precisely the kind of effect expected from the existence of an unmodeled component with an approximately constant spectral profile across test samples.

The detailed statistical analysis is shown in Table 2 in terms of average prediction error for both PARAFAC and BLLS and at both working pH values, including the relevant information employed for data processing. Inspection of Table 2 seems to indicate similar predictive abilities for both algorithms. However, better insight is gained by studying the EJCR of the regression of predicted versus nominal analyte concentrations. The corresponding plots are shown in Figure 6: all confidence regions contain the ideal point of unit slope and zero intercept (indicating accuracy), but the elliptic sizes are apparently different. The ellipses for pH 4.0 are smaller than for pH 6, suggesting that the chemometric methodologies show better predictive ability when the number of species is smaller. However, BLLS displays smaller EJCR at both working pH as compared to PARAFAC, pointing to an improved analytical precision of the former. For comparison, the highly biased elliptical regions for N-PLS are also included in Figure 6. In this latter case, the region at pH 4.0 is smaller than

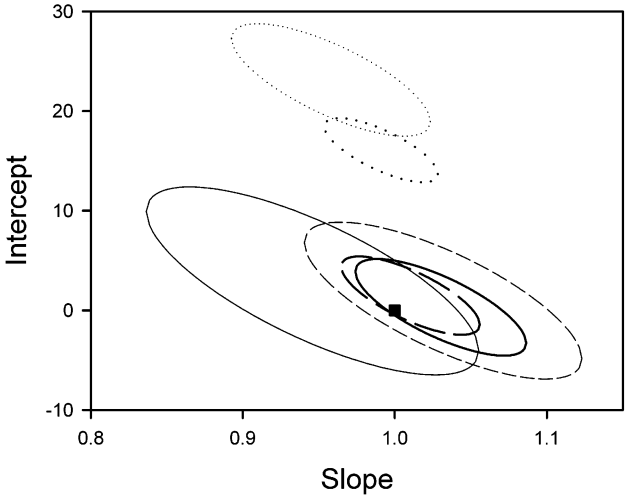

Figure 6. Elliptical joint confidence regions for the slope and intercept of the regression of predicted concentration vs nominal values in the test set: (—) PARAFAC, (– –) BLLS, and (· · ·) N-PLS. The thick lines correspond to the results at pH 4.0, the narrow lines at pH 6. The solid square marks the ideal (1,0) point.

at pH 6; however, the lack of accuracy at both pH values is apparent for this technique, because the EJCRs do not contain the ideal (1,0) point.

Average sensitivities and selectivities for PARAFAC and BLLS over the analyzed test set under the studied conditions are also listed in Table 2. They are similar for both algorithms at pH 4.0 but significantly differ at pH 6. In the latter case, BLLS shows considerably better figures than PARAFAC, due to lower spectral overlapping. This fact may help to explain the BLLS enhanced predictive ability toward the analyte in the spiked sample set.

The limits of detection computed with the approximate eq 24 are also reported in Table 2. They are probably too optimistic, because they do not include calibration uncertainties but give an overall idea of the quality of the presently applied techniques: in the worst possible scenario, the LOD is $\sim 5\ \mu g\ L^{-1}$, which can be translated into an LOD of 5 mg L^{-1} for the original urine samples (due to the dilution factor of 1:1000). This latter value is a sensible estimation of the LOD, given the predicted analyte concentrations for the blank urines T15—T18 (Table 1).

Real Samples. The analysis of four real samples (R1—R4 in Table 3) was performed under both working conditions, i.e., by processing with both algorithms the EEM data recorded at pH 4.0 and also at pH 6. Table 3 shows that the predicted concentrations are statistically comparable to those found by liquid chromatography, indicating that second-order fluorescence is a valid methodology for ciprofloxacin monitoring in urine. The comparison is based on a paired-*t* statistics (Table 3). The PARAFAC predicted values appear to be closer to those found by HPLC at pH 4.0 than at pH 6, whereas no definite trend if found in the BLLS predictions at both pH values.

Table 3. PARAFAC, BLLS and HPLC Results for Real Urine Samples[a]

	PARAFAC		BLLS		
sample	pH 4.0	pH 6[b]	pH 4.0	pH 6	HPLC
R1	256	278	265	268	265
R2	214	219	186	205	200
R3	186	185	182	186	196
R4	252	258	237	244	240

[a] All results are expressed in mg L^{-1}. For a paired *t*-test comparison between each of the chemometric methods and HPLC, average standard error, 8 mg L^{-1} (obtained by replicate analysis); degrees of freedom, 2; confidence level, 95%; critical *t* value, 4.3. Values of (Δ/SE) are all smaller than the critical *t* (Δ is the difference between the results under comparison). [b] Values were computed using data for the most sensitive prototropic $H_2(CIP)^+$ form.

Method Comparison. In comparing second-order multivariate methodologies, one should take into account the following characteristics: (1) analytical performance, (2) model interpretability, and (3) ease and speed of program operation.

Both BLLS and PARAFAC are able to handle the occurrence of interferences not modeled in the calibration set, a property of immense utility in the analytical context (notice that the popular N-PLS algorithm does not provide adequate results for the present problem, because it does not exploit the second-order advantage). These two methods also yield spectral properties of useful physical meaning. The results discussed in the present report indicate that under certain circumstances, however, the interpretability of PARAFAC results is of superior quality, providing the correct spectral profiles for equilibrating acid—base species. However, the focus of BLLS is on prediction rather than on interpretation, and from this point of view its analytical performance can be considered to be better, both in accuracy and precision, at least concerning the presently studied system.

As regards computer operation, all methods can be programmed in MATLAB and introduced into a friendly, user-interface mode, and hence, no significant differences can be established in this respect. However, BLLS seems to be simpler as regards constraining options and number and quality of tunable parameters for program initialization.

ACKNOWLEDGMENT

Financial support from CONICET (Consejo Nacional de Investigaciones Científicas y Técnicas), Universidad Nacional de Rosario, Agencia Nacional de Promoción Científica y Tecnológica (Project PICT 99 06-06078) and Universidad Nacional del Litoral (Project FOMEC-Quimica 129 UNL) is gratefully acknowledged. We also thank Sanatorio Santa Fe (Santa Fe, Argentina) for providing the real urine samples.

Received for review December 30, 2003. Accepted March 5, 2004.

AC035541W